INTENSIVE EVAPORATION AND BOILING OF A HETEROGENEOUS LIQUID DROPLET WITH AN EXPLOSIVE DISINTEGRATION IN HIGH-TEMPERATURE GAS AREA

by

Maxim V. PISKUNOV, Pavel A. STRIZHAK*, and Anastasia A. SHCHERBININA

National Research Tomsk Polytechnic University, Tomsk, Russia

Original scientific paper
DOI:10.2298/TSCI150418164P

The using of the high-speed (not less than 10^5 frames per second) video recording tools (Phantom) and the software package (TEMA Automotive) allowed carrying out an experimental research of laws of intensive vaporization with an explosive disintegration of heterogeneous (with a single solid non-transparent inclusion) liquid droplet (by the example of water) in high-temperature (500-800 K) gases (combustion products). Times of the processes under consideration and stages (liquid heat-up, evaporation from an external surface, bubble boiling at internal interfaces, growth of bubble sizes, explosive droplet breakup) were established. Necessary conditions of an explosive vaporization of a heterogeneous droplet were found out. Mechanisms of this process and an influence of properties of liquid and inclusion material on them were determined.

Key words: *evaporation, explosive vaporization, heterogeneous liquid droplet, solid inclusion, high-temperature gas area*

Introduction

The fire extinguishing technologies by atomization of liquid compositions (*water mist, water fog, water curtain*) as a rule, are based on the supply of finely divided droplet flow into the combustion area [1-5]. Under these conditions, the emphasis is upon the decrease of droplet sizes (up to several tens of micrometers) and the increase of droplet number in a flux to rise the evaporation area [1-5]. The experimental researches [5-7] carried out in recent years illustrated that in case of typical fires, the probability of small droplet entrainment by high-temperature combustion products from the burning area is high. As a consequence, it is expedient to increase the droplet sizes when introducing into the flux of combustion products. At the same time, the droplet heat-up should be accelerated to intensify the vaporization in the burning area.

The approach to intensify the droplet heat-up of extinguishing liquid in the burning area by addition of solid inclusions into droplets illustrated that the mass velocities of vaporization can be significantly increased by addition of nontransparent particles (as an example of carbon, graphite, and aluminum) [5]. The experimental researches [7] carried out by using the modern panoramic optical methods (PIV [8], IPI [9], SP [10]) allowed determining the characteristic evaporation speeds of heterogeneous droplets. According to the results of experi-

* Corresponding author; e-mail: pavelspa@tpu.ru

ments [7], it was made an assumption that the intensification of vaporization takes place not only at a free surface of heterogeneous droplet but at internal solid inclusion/liquid interface. As follows, from the theoretical analysis of the experiment results [7] with heterogeneous liquid droplets in high-temperature gas areas, it was hypothesized that the conditions of an explosive vaporization inside the droplet and its destruction can be reached by addition of solid inclusion into liquid droplet. This effect will allow increasing the evaporation area of liquid composition within the actual fire situation zone in several times. At first the insufficient study of this effect can be explained, as a rule, by difficult [11, 12] processes of the formation and growth of bubbles at internal interfaces, high speeds of processes at intensive heat exchange – especially at the typical (more than 600 K) temperatures of fires, possible vaporization at external surface and internal interfaces. Currently, there are not any even simplified models to predict the conditions of an explosive vaporization of heterogeneous droplets.

The aim of this work is to establish experimentally the main laws of an explosive vaporization of heterogeneous (with solid particles) droplets of water in the combustion product flux which corresponds to the actual fire situations and to develop the predictive model of heat transfer.

Experimental set-up and methods

While researching, the set-up (fig. 1) was used which was similar by the main elements to experiments [5-7]. High-speed video recording of heterogeneous droplet evaporation at the rod (3) (material – ceramic) was carried out. Two high-speed (to 10^5 fps) video cameras (Phantom V411 and Phantom Miro M310) (11) were used. The cameras were located on the 90° angle relative to each other. As a result, 3-D picture of an evaporating droplet was created. It allowed determining 3-D droplet sizes. A heterogeneous droplet was fixed into the channel

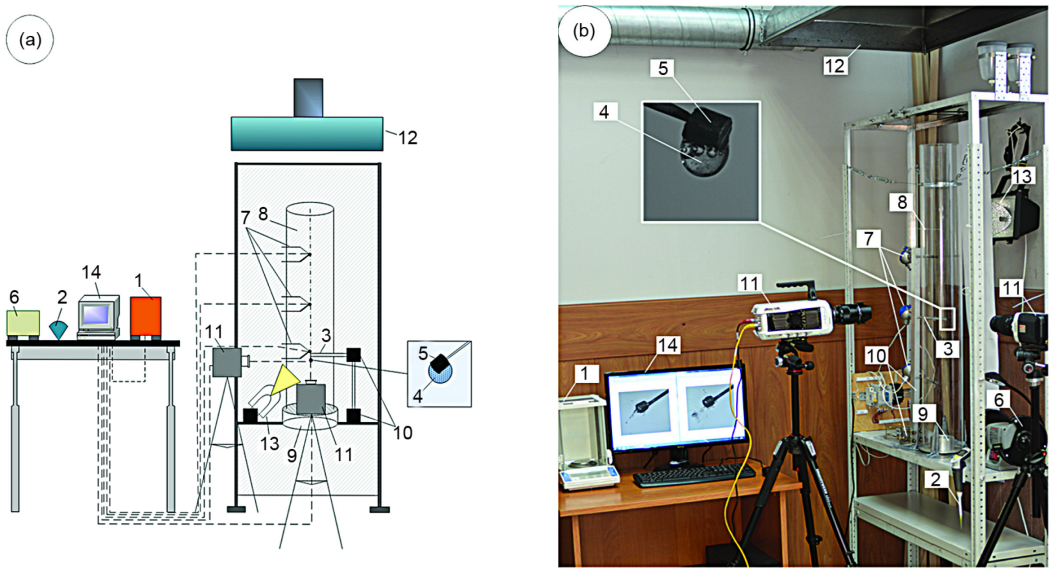

Figure 1. A scheme (a) and physical configuration (b) of the experimental set-up
1 – analytical weighing system, 2 – electronic dosing devise, 3 – rod (holder for inclusion), 4 – droplet, 5 – inclusion, 6 – complex to manufacture inclusions, 7 – thermocouples, 8 – cylinder of quartz glass, 9 – burner, 10 – moving mechanisms, 11 – high-speed cameras, 12 – plenum system, 13 – spotlight, 14 – personal computer (PC)

of cylinder (8) (material – quartz glass, height 1 m, internal and external diameters – 0.2 m and 0.206 m) which was full of combustion products of industrial alcohol. The frames of videograms from two cameras were processed on PC (14) by using *TEMA automotive and phantom camera control* software.

The burner (9) was placed at the base of the cylindrical channel (8). An industrial alcohol, which was used later to generate high-temperature gases, was filled in the burner (9). The choice of an industrial alcohol as a combustible liquid is due to less smoke generation ability in comparison with kerosene used in experiments [5-7]. On account of this, the sufficient droplet image contrast was provided during the video registration.

Three technologic holes were done in the cylindrical channel (8) (at a height of 0.3, 0.5, and 0.7 m relative to the base of burner (9) to fix the chromel-alumel thermocouples (7) (measuring temperature range 273-1373 K, measurement error ±3.3 K) and to insert the ceramic rod (3) with a fixed heterogeneous droplet (4) into the channel (8) (after measurement of gas area temperature). The temperature of the gas area in the experiments was changed in the range of 500-800 K by the air flow regulation through special holes in the burner (9) and the operation parameter variation of plenum system (12). The injection of the rod (3) with a heterogeneous droplet was carried out into one of three holes in the channel (8) according to required temperature of gas area. The initial temperature of droplets and inclusions corresponded to the temperature of air in the laboratory room (about 290 K).

Graphite was chosen as the material of solid non-metal inclusion (5). The complex (6) was used to produce the inclusion in the form of cylindrical disk with fixed sizes (radius 1 mm, height 2 mm) and parallelepiped ($a \approx 1$ mm, $b \approx 1$ mm, and $c \approx 2$ mm). The hole with a radius 0.15 mm and a depth not more than 0.3 mm was done in the particle along the symmetry axis. Using this hole, the carbon particle was fixed on the ceramic rod (the length about 0.25 m). The inclusions in the form of cylindrical disk and parallelepiped were chosen because of some reasons. Firstly, such configuration and small technological hole are minimized (in comparison with sphere) the influence of rod on the conditions of heterogeneous droplet heat-up (there is no contact between water and rod). Secondly, the pilot experiments with inclusions in the form of sphere, parallelepiped, ellipsoid and disk illustrated that the liquid covered steadily the inclusion in the non-spherical form.

The routine of experiments included several stages. At the preliminary stage, the intake of distil water droplet was carried out from the vessel by the electronic one-channel dosing device (2) (*Finnpipette novus*: minimum taken volume – 5 μl, maximum taken volume – 50 μl, and variation step – 0.1 μl). Then, the weighing was carried out by using the analytical weighing system (1) (VIBRA AF 225DRCE: maximum weight – 220 g, minimum weight – 0.001 g, and error – not more than 0.5% of measuring weight). The mass of liquid droplets was varied in the range of 5-20 mg by the change of electronic dosing device (2) parameters. After weighing, the intake of water droplet from the base of analytical weighing system (1) was carried out. The droplet of fixed mass was lowered on the graphite inclusion fixed on the rod (3) by using the adapter of dosing device (2). The movement of ceramic rod (3) was performed in two co-ordinates (along the symmetry axis of cylinder 8 and perpendicular to axis at the insertion of droplets into high-temperature gas area) by using the automated moving mechanisms (10). After movement of the rod (3) with heterogeneous droplet into a gas area, the video recording of droplet evaporation was implemented. The spotlight (13) was applied to improve the contrast of droplet image, the identification of interfaces in a droplet and liquid film thickness. The obtained video materials were processed on PC (14) by using the *TEMA automotive* software: the scale factor was calculated by two fixed points, the distance between

which was known (the preliminary video recording of calibration target was implemented), the sizes of droplet (maximum sizes in three co-ordinate directions and then the average d was calculated) and liquid film thicknesses (on each edge of particle δ) on an inclusion were determined. The measurements of droplet sizes and film thickness were carried out to record the location of water evaporation surface.

Video recording with the fixation of change of droplet sizes and film thickness was continued in each experiment until complete water evaporation (film thickness did not exceed the value comparable to the error of measuring instruments) or *explosion* (disintegration) of droplet on a few droplets of significantly smaller sizes. The lifetime τ_h of heterogeneous droplet (heating until explosive disintegration or complete evaporation in the form of single droplet) were determined for recorded video by using *Phantom camera control* software. Errors in size measurements of inclusion, water droplet and film thickness did not exceed 0.01 mm. Repeatability of d and δ determination was 7%. Errors on life times (τ_h and τ_e) determination were 1 ms.

Results and discussion

As a result of conducted experiments, it was established that the vaporization of heterogeneous liquid droplets under considered conditions can be according to one of three schemes. At first, their realization depends on gas temperature and characteristics of the inclusion covering by liquid. The experiments illustrated that the liquid lowered by the dosing device can cover the inclusion fully when water mass is less than 7 mg. In case of larger mass, the liquid dripped under gravitational force action and the form of parachute is observed.

The 1st established scheme of vaporization corresponds to liquid evaporation from a free droplet surface only. In this scheme, the temperatures up to 600 K are characteristic. Figure 2 illustrates the typical video frames with heterogeneous droplet at about 500 K at different times.

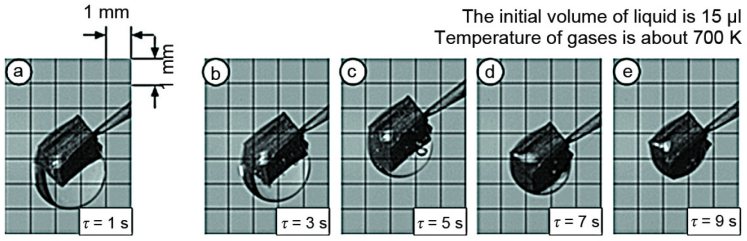

Figure 2. Photos of water droplet with inclusion during vaporization according to the first scheme

The significantly non-uniform decrease of liquid film thickness can be noted both during the time and along the inclusion surface. At first, this is due to significantly non-linear dependence of liquid evaporation rate on temperature.

When realizing the 1st scheme the conditions of intensive vaporization at internal interfaces were not reached. In singular experiments, the cases of the formation of several bubbles at these interfaces were recorded. But their lifetimes were too small – significantly smaller than times of realization of the liquid evaporation process.

The 2nd scheme (fig. 3) was established for water droplets with single inclusions fully-submerged in them. The realization of this scheme depended on the liquid film thickness around the inclusion. The 1st scheme was realized, when the thickness was less than 0.2 mm independent from gas temperature. The vaporization was according to the 2nd scheme at the large thicknesses of film and more than 700 K.

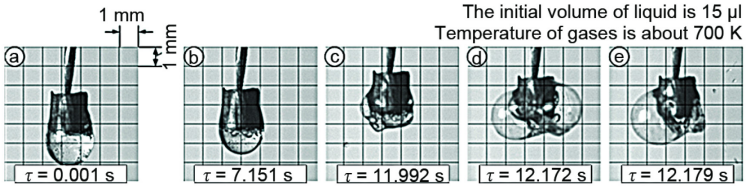

Figure 3. Photos of water droplet with inclusion during vaporization according to the second scheme

The 2nd scheme included the following stages. The 1st stage is heat-up of a liquid film around the inclusion until the achievement of conditions of intensive vaporization at internal interfaces. This stage, like everything else, is followed by water evaporation from a free droplet surface. The decrease of droplet sizes at evaporation can be explained by the influence of this factor. The formation of bubbles was recorded after a few seconds from the beginning of droplet heating on the inclusion surface. However, this process can not be called as high-speed or characterized by a sharp increase in the number and sizes of bubbles. They are formed not even over the inclusion. But explosive droplet destruction has occurred after a short time interval (as a general, less than 1 second) from the beginning of first bubble formation. Totally, the process of explosive vaporization was not more than 10 seconds according to the 2nd scheme at variation of gas temperatures from 700-800 K.

The 3rd scheme corresponded to conditions of partial protrusion out of the droplet surface (fig. 4). This scheme was realized at gas temperatures more than 650 K and characterized by the minimum duration in comparison with two other schemes.

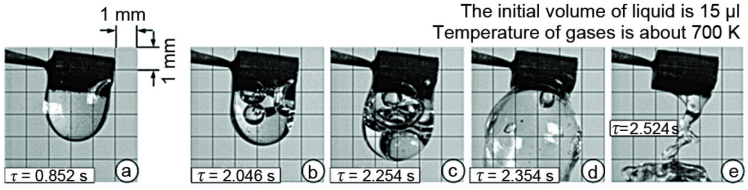

Figure 4. Photos of water droplet with inclusion during vaporization according to the third scheme

The 3rd scheme included the processes of water evaporation from a free surface of heterogeneous droplet similar to the first two schemes. But the process of vaporization on internal surfaces dominated at realization of considered scheme as opposed to the 1st and 2nd ones. It is very important to note the increase of droplet sizes relative to initial (in many cases even in several times) ones due to bubble growth (fig. 4). Such effect was not recorded at two other schemes. At first, this is due to intensive energy supply to the internal interfaces through the inclusion at its heating by gases and through the liquid. The energy through the liquid was supplied to the inclusion boundary and accumulated in a thin boundary layer by radiant heat transfer and water transparency, but if through the inclusion – by conductive heat transfer.

Only in the 3rd scheme the bubbles formed at the interface are departed intensively and merged with neighbor ones. The significant increase of droplet size and filling of the major part of its volume by liquid vapors can be explained by this fact. As a consequence, droplets become sufficiently non-stable at such dynamic change of sizes. Furthermore, the liquid film thickness decreases multiply when the sharp increase of droplet sizes due to vaporization at internal interfaces. This decreases significantly the liquid pressure in comparison with pressure of vapors in-

side the droplet. As a consequence, the processes of its explosive destruction (fig. 4), which became typical for considered conditions, were recorded after the droplet size increase.

It can be noted that *explosions* of droplets at temperatures from 650-800 K were recorded sufficiently steadily. When increasing the gas temperature, the established effect was more evident and clear. The gas temperature level (about 800 K) limited for conducted experiments is due to that fact that the changeover to more caloric fuels was accompanied by combustion product formation, part of which disturbed during the recording in consequence of bad or full (soot) non-transparency. For this reason, the temperature range extension of gas area, which is external in relation to droplet, is not possible yet. But it can be supposed that the times of droplet heat-up until explosive destruction will be decreased because of the growth of radiant heat flux to heterogeneous droplet surface when increasing the temperature of gases heating the heterogeneous transparent water droplet according to the analysis and the compilation of experiment results.

Three emphasized schemes of vaporization allowed proving the effect on which the decrease of droplet sizes due to evaporation can be followed within the 1st scheme only. This is due to bubble boiling mostly in the 2nd and 3rd schemes. The formation and growth of bubbles lead to some *swelling* of the droplet. According to the 3rd scheme this *swelling* is significant, at the 2nd scheme it is moderate, but it was recorded too.

Figure 5(a) illustrates the times of complete liquid evaporation within the 1st vaporization scheme (without explosive destruction of the droplet).

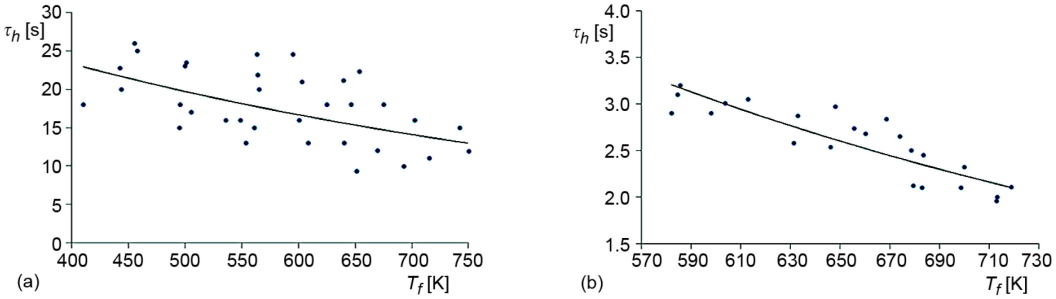

Figure 5. Times of complete liquid evaporation from free surface of heterogeneous droplet (a) and explosive vaporization of droplets (b) at different gas temperatures: the initial volume of water is 15 μl

The obtained dependences correspond closely to the conclusions of experimental researches [5-7] of droplet evaporation processes with a group of inclusions. Gas temperature, concentrations, and inclusion sizes are emphasized as the main factors. In the present work, the gas temperature is the determining factor for a scheme and duration of vaporization.

Figure 5(b) illustrates the lifetimes of heterogeneous droplets until the conditions of explosive vaporization. Primarily, the durations, which are significantly different (smaller) in comparison with the durations presented in fig. 5(a) can be noted. This effect is the main one characterizing explosive droplet destruction.

The emphasized features at the realization of three schemes of heterogeneous water droplet vaporization are of interest for two-phase and heterogeneous systems, for example, [13-15]. The analysis of results [5-7] and the present work illustrated that the probability of explosive droplet destruction is minimal, when the inclusion sizes are multiply smaller in comparison with a droplet. This effect at comparably sized (not less than 50% of droplet volume) inclusions is the most probable under conditions of high (more than 650 K) tempera-

tures. As a consequence, the corresponding sizes of inclusions and heterogeneous droplets can be recommended depending on required effect.

Also it can be noted that the second and 3rd schemes of vaporization illustrate the fairly different initial conditions, which are necessary and sufficient for *explosions* in high-temperature heterogeneous gas-droplet applications. In accordance with the 1st scheme (at complete immersion of inclusion into water), the special preparation of heterogeneous droplets is necessary. It is expedient to choose the inclusions with low thermal conductivity (to accumulate the supplied energy in a small boundary layer near internal interfaces) to enhance the *explosion* effect. In case of the 3rd scheme, *vice versa*, it is expedient to choose the inclusion material with high (more than for liquid) thermal conductivity to accelerate energy supply to internal interfaces.

The model of heat and mass transfer can be formulated by analyzing the results of phase transformation features of heterogeneous water droplet in high-temperature gases, which were established in the conducted experiments. Its main purpose is to predict conditions of explosive vaporization at internal interfaces in a heterogeneous droplet at the intensive heating (experimental researches of all possible factors, effects, and influence of parameters will require the rather more resources in comparison with mathematical simulation). Therefore, it is expedient to make the simple model to provide the possibility of its application by the wide range of specialists. The data analysis of carried out experiments illustrated that, firstly, the developing model should take into account the processes of heat transfer, including conductive and radiant mechanisms, the heat sinks at phase transformations and radiation absorption, as well as the formation of a buffer vapor layer between liquid film and inclusion. Taking into account these factors, the formulated physical and mathematical models are presented in the next sections.

Model and results of numerical simulation

The 1-D axially symmetric scheme was used while formulating the physical statement of simplified heat transfer model. It was recognized that the inclusion was covered around by liquid (the film had the uniform thickness) at the initial time. Initial temperatures of liquid and inclusion (T_0 = 300 K) were significantly less than the temperature of the gas area (T_f = 600-1500 K). Similar to the carried out experiments, graphite was regarded as the material of inclusion, gas area was combustion products of industrial alcohol, liquid was distil water.

At T_0 and T_f, the heat-up of liquid occurred by conductive and radiant heat transfer taking into account endothermal phase transformations at inclusion/liquid and liquid/gas interfaces. These phase transformations lead to the decrease of water film thickness around the inclusion. As a consequence, droplet size is decreased and thickness of the buffer vapor layer is increased. The biggest part of energy is accumulated at the inclusion/vapor interface by the heat supplied by gas area and its passing into heterogeneous droplet (in consequence of transparency of liquid and vapors). This leads to the sharp increase of temperature at this interface. The buffer vapor layer is heated intensively owing to its thickness. This leads to the domination of endothermal transformations at internal interfaces in a droplet in comparison with transformations at the free surface. Under conditions of intensive vaporization, the pressure of vapors inside a droplet exceeds significantly the pressure caused by surface tension force of liquid and gas area.

While stating the problem, it was accepted that the conditions of explosive vaporization were possible, when values of temperatures (at interfaces) corresponded to liquid boiling (for water $T \approx 370$ K). The time of heterogeneous droplet heating until the achievement of in-

tensive vaporization, $T(R_1) \approx 370$ K was calculated from the results of the problem solution. This time was the explosive vaporization time of heterogeneous droplet, τ_h. This is due to the fact that the processes of intensive formation and growth of bubbles at internal interfaces preceded the explosive droplet destruction in the 2nd and 3rd schemes, emphasized in conducted experiments. These processes illustrated the boiling, which was possible at high temperatures of inclusion surface, in particular, $T(R_1) \approx 370$ K.

The following system of non-linear non-stationary equations with partial derivatives ($0 < \tau \le \tau_h$) was used to simulate the described processes:

– inclusion $0 < R < R_1$

$$c_1\rho_1 \frac{\partial T_1}{\partial \tau} = \lambda_1 \left(\frac{\partial^2 T_1}{\partial R^2} + \frac{2}{R} \frac{\partial T_1}{\partial R} \right) \tag{1}$$

– buffer vapor layer $R_1 < R < R_2$

$$c_4\rho_4 \frac{\partial T_4}{\partial \tau} = \lambda_4 \left(\frac{\partial^2 T_4}{\partial R^2} + \frac{2}{R} \frac{\partial T_4}{\partial R} \right) + \frac{\partial H_4(R)}{\partial R} \tag{2}$$

– liquid film $R_2 < R < R_3$

$$c_2\rho_2 \frac{\partial T_2}{\partial \tau} = \lambda_2 \left(\frac{\partial^2 T_2}{\partial R^2} + \frac{2}{R} \frac{\partial T_2}{\partial R} \right) + \frac{\partial H_2(R)}{\partial R} \tag{3}$$

Initial ($\tau = 0$) conditions: $T = T_0$ at $0 < R < R_2$.

Boundary conditions at $0 < \tau \le \tau_h$:

$$R = 0, \quad \frac{\partial T_1}{\partial R} = 0 \tag{4}$$

$$R = R_1, \quad \lambda_4 \frac{\partial T_4}{\partial R} = \lambda_1 \frac{\partial T_1}{\partial R} - H(R_1) \tag{5}$$

$$R = R_2, \quad \lambda_2 \frac{\partial T_2}{\partial R} = \lambda_4 \frac{\partial T_4}{\partial R} + Q_e W_e(T) \tag{6}$$

$$R = R_3, \quad \lambda_2 \frac{\partial T_2}{\partial R} = H(R_3) - Q_e W_e(T) \tag{7}$$

The mathematical expressions of the Stefan-Boltzmann and Bouguer-Lambert-Beer laws were used to calculate the heat-flux density:

$$H(R_3) = \varepsilon_2 \sigma [T_f^4 - T(R_3)^4] \tag{8}$$

$$H(R_2) = H(R_3) \exp[-k_{\lambda 2}(R_3 - R_2)] \tag{9}$$

$$H(R_1) = H(R_2) \exp[-k_{\lambda 4}(R_2 - R_1)] \tag{10}$$

$$H_2(R) = H(R_3) \exp[-k_{\lambda 2}(R_3 - R)], \quad R_2 < R < R_3 \tag{11}$$

$$H_4(R) = H(R_2) \exp[-k_{\lambda 4}(R_2 - R)], \quad R_1 < R < R_2 \tag{12}$$

where indexes 1, 2, 3, and 4 correspond to an inclusion, liquid, gases, and vapors in eqs. (1)-(12).

The size of buffer vapor layer ($R_2 - R_1$) and the total size of droplet (R_3) were calculated by using the approach [16-18] based on applying the group of expressions taking into account the dynamic pressure of vapors, pressure of liquid, and external area. Depending on a difference of these pressures the necessary thickness ($R_2 - R_1$) of buffer vapor layer was determined by iterations to provide the balance of pressures [18]. This pressure balance of vapors and liquid film provided the integrity of liquid film around an inclusion.

The evaporation speeds, W_e, at inclusion/liquid and liquid/gas interfaces were determined by using the dependence established resulting from experimental data processing [17]: $W_e(T) = 5 \cdot 10^{-5} \exp 0.02T$.

It was established in the carried out experiments that the energy can be supplied to internal interfaces through inclusion and liquid. To estimate the influence of this effect on conditions of explosive vaporization in the model, the boundary condition (4) was changed:

$$R = 0, \quad \lambda_3 \frac{\partial T_3}{\partial R} = \lambda_1 \frac{\partial T_1}{\partial R} - H(R_0) \tag{13}$$

$$H(R_0) = \varepsilon_1 \sigma [T_f^4 - T(R_0)^4].$$

Equation (13) accounted the energy supply to inclusion from the gas area directly (without liquid film).

The system of eqs. (1)-(13) was solved by finite difference method [19]. The discretized equations were solved by iterations [19]. The sweep method using an implicit four-point difference scheme [19] was applied to solve 1-D difference equations. The reliability of numerical research results is determined in several steps. Firstly, calculation examples show that when the time step or mesh size decreases by a factor of 10 and 2, respectively, the numerical results vary by less than 0.5%, which justifies the used time step and mesh sizes [15, 16]. Secondly, it is provided from a perfect agreement between the modelled and experimental results.

The initial temperature of water droplet with solid inclusion (T_0 = 300 K), external gaseous area (T_f = 600-1500 K), initial droplet size (R_1 = 0.5–2 mm), initial liquid film thickness (δ = 0.1–1 mm) were the initial data at numerical simulation. The thermal and physical characteristics of carbon particle, distil water, combustion products of industrial alcohol, and optical properties of liquid and inclusion were chosen according to [20-22].

The features of heat transfer of different vaporization schemes were established by the results of conducted numerical simulation. In particular, it was able to establish the influence of the effect of vapor layer formation between liquid film and inclusion on the vaporization conditions at numerical simulation, to analyze the physical differences of energy supply to internal interfaces through inclusion and liquid, to emphasize the role of radiant heat transfer in heterogeneous droplet.

Figure 6(a) illustrates the temperature distributions of liquid during its heating in high-temperature gas area (it was considered the case without formation of the buffer vapor layer between inclusion and liquid). The significantly non-uniform heat-up (over the thickness) of liquid film can be noted. This is due to the substantial impact of phase transformations at interfaces and the determining role of the radiant heat transfer in a droplet. In particular, it is clearly seen, see fig. 6(a), that the temperature at inclusion/liquid interface growths faster than over the liquid film thickness.

The distribution of temperatures is changed significantly, see fig. 6(b), when forming the vapor layer between the liquid and inclusion. Primarily, the significant decrease of inclusion surface heat-up times until temperatures, providing the liquid boiling at internal interfaces and explosive vaporization can be noted. This is due to the fact that the accumulation of

radiant thermal flux of gas area and the energy consumption for endothermal phase transformation occur at different interfaces (inclusion/vapor and vapor/liquid). Since the liquid and vapor are transparent and inclusion is non-transparent, the main part of radiant thermal flux is accumulated at the surface of inclusion. The formation and growth of layer lead to vapor/liquid boundary displacement from interface to droplet surface. This leads to the intensification of vapor heat-up in a small wall boundary layer and, as a consequence, the increase of vapor pressure in this area. The explosive vaporization times are significantly smaller than in heterogeneous droplet without regard to the vapor layer at internal interfaces.

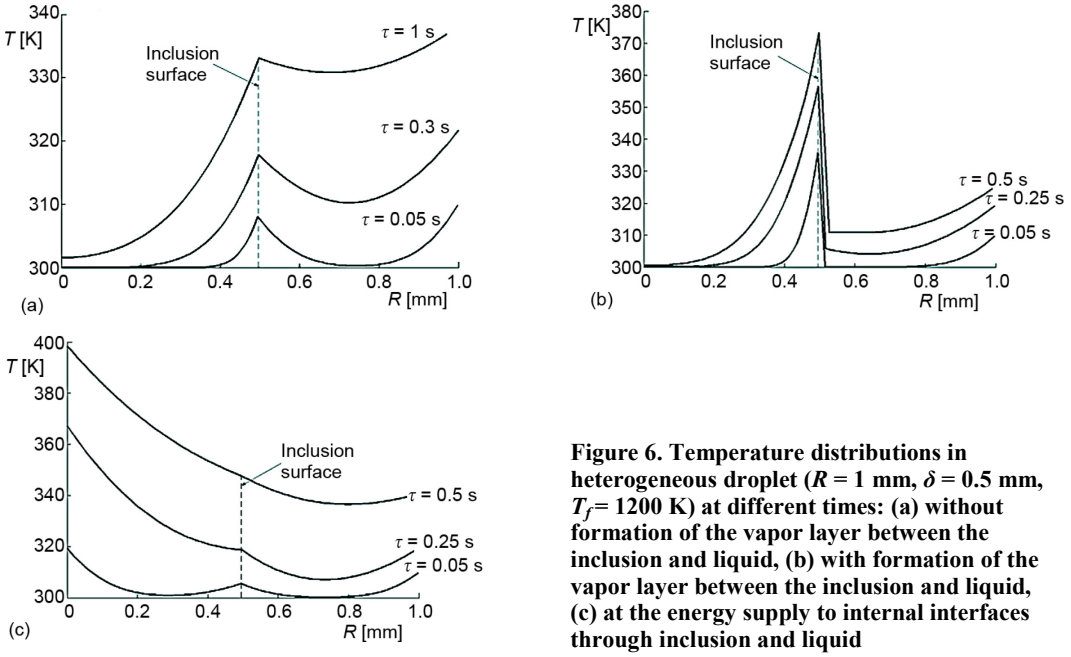

Figure 6. Temperature distributions in heterogeneous droplet (R = 1 mm, δ = 0.5 mm, T_f = 1200 K) at different times: (a) without formation of the vapor layer between the inclusion and liquid, (b) with formation of the vapor layer between the inclusion and liquid, (c) at the energy supply to internal interfaces through inclusion and liquid

Figure 6(c) illustrates the temperature distributions in heterogeneous droplet while realizing the 3rd scheme established in experiments (*i. e.* at the energy supply to internal interfaces through inclusion and liquid). The energy of the external gas area is supplied faster through the inclusion to the particle/liquid interface, see fig. 6(c), by the reason of higher thermal conductivity of inclusion in comparison with liquid and vapor. This leads to the intensification of phase transformations at this interface during shorter time than at the heat-up through the liquid film around the inclusion only. This result explains the shorter times, τ_h, while realizing the 3rd scheme in comparison with the 2nd one in the conducted experiments (fig. 7). Also, this can explain the smaller values of limited gas temperatures, at which explosive vaporization takes place (fig. 7).

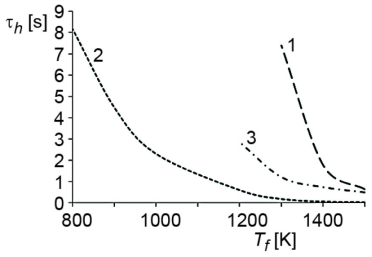

Figure 7. Numerical values of explosive vaporization times for different models
1 – without vapor layer, 2 – with vapor layer, 3 – at energy supply to interface through inclusion and liquid

The dependences presented in fig. 7 allow concluding about the important role of thermal and physical characteristics of inclusion material. When the thermal

conductivity of inclusion is higher than liquid, the times, τ_h, could be decreased by larger protrusion of inclusion over the droplet surface (most of gas energy will be supplied to internal interfaces through a particle rather than liquid). When the thermal conductivity of inclusion is less than liquid, it seems expedient to use another effect – the accumulation of energy, passing through the liquid, near the surface of non-transparent inclusion (these conditions correspond mostly to the 2nd scheme of vaporization, which was established in the conducted experiments).

The physical features emphasized while simulating, can explain the minimum temperatures of gases, at which explosive vaporization is possible for different models. In particular, fig. 7 illustrates that the explosive vaporization is realized even at about 800 K at energy supply to the internal interface through the inclusion and liquid. The minimum temperatures of gases are higher than this value (1200 K and 1300 K, correspondingly) for two other models. However, the minimum gas temperatures established during the simulation and which are sufficient for explosive vaporization, correspond to the temperatures from experiments (especially, if the model with energy supply to the interface through inclusion and liquid is taken into consideration). It is evident that the close agreement of theoretical and experimental results in this case can be reached by the development of 2-D or even spatial models taking into account the main processes of heat- and mass transfer. Also, the satisfactory fit of limited temperatures of gases in experiments and models can be reached at the correction of required temperature at internal interfaces for explosive droplet destruction (it was temperature about 370 K in the present work, it can be lower in actual practice – for example, about 340-350 K; as a consequence, the times, τ_h, and gas temperatures will be decreased to times and temperatures emphasized in the experiments). Unfortunately, the approaches and experimental methods for reliable measurement of temperature at internal interfaces during intensive vaporization have not been developed yet. But the models, presented in this work, can be applied to predict and estimate explosive vaporization conditions, stages and mechanism of this process.

The carried out numerical and experimental investigations illustrated that the explosive destruction of heterogeneous droplets in high-temperature gas areas was possible by intensive vaporization. It was realized with high stability at high temperature of gases. As a consequence, this effect can be applied in various gas-vapor-droplet technologies (examples are: thermal or flame cleaning of water; gas-vapor-droplet heat carriers; processing of power engineering equipment surfaces; fire extinguishing by using special heterogeneous mixtures and aerosols) at intensification of vaporization.

Conclusions

The carried out research allowed recording the conditions of explosive destruction of a heterogeneous droplet in high-temperature gas area. It was established that large heat fluxes to inclusion/liquid interface are the necessary conditions for this effect. The conducted experiments illustrated that two schemes of droplet explosion with different processes of energy supply to internal interfaces and one scheme of intensive evaporation from a free surface of heterogeneous droplet were possible. The established laws allowed developing the physical and mathematical models of heat and mass transfer taking into account the formation of vapor layer between liquid film and inclusion. The prediction of the main parameters influence of studying process on explosive vaporization times was carried out by using this model. The created model can be applied to analyze the necessary and sufficient conditions of explosive droplet vaporization of various heterogeneous liquids under conditions of intensive heat ex-

taking into account various inclusion shapes and its location in a droplet according to the features established in the conducted experiments is appropriate.

Acknowledgment

This work was supported by the grant of the President of the Russian Federation (MD-2806.2015.8).

Nomenclature

c – thermal capacity, [Jkg^{-1}K^{-1}]
$H(R)$ – density of heat-flux, [Wm^{-2}]
k_λ – coefficient of power adsorption, [–]
Q_e – heat of phase transformation, [Jkg^{-1}]
R – radial co-ordinate, [mm]
T – temperature, [K]
T_0 – initial temperature, [K]
T_f – temperature of gas area, [K]
W_e – evaporation rate, [kgm^{-2}s^{-1}]

Greek symbols

δ – liquid film thickness, [mm]
ε – emissivity factor, [–]
λ – thermal conductivity, [Wm^{-1}K^{-1}]
ρ – density, [kgm^{-3}]
σ – Stefan-Boltzmann constant, [Wm^{-2}K^{-4}]
τ – time, [s]
τ_h – lifetime of heterogeneous droplet, [s]

References

[1] Xiao, X. K., *et al.*, On the Behavior of Flame Expansion in Pool Fire Extinguishment with Steam Jet, *Journal of Fire Sciences*, *29* (2011), 4, pp. 339-360
[2] Yao, B., Cong, B. H., Experimental Study of Suppressing Poly(methyl methacrylate) Fires Using Water Mists, *Fire Safety Journal*, *47* (2012), Jan., pp. 32-39
[3] Tang, Z., *et al.*, Experimental Study of the Downward Displacement of Fire-induced Smoke by Water Spray, *Fire Safety Journal*, *55* (2013), Jan., pp. 35-49
[4] Joseph, P., *et al.*, A Comparative Study of the Effects of Chemical Additives on the Suppression Efficiency of Water Mist, *Fire Safety Journal*, *58* (2013), May, pp. 221-225
[5] Volkov, R. S., *et al.*, Influence of Solid Inclusions in Liquid Drops Moving through a High Temperature Gaseous Medium on Their Evaporation, *Technical Physics*, *59* (2014), 12, pp. 1770-1774
[6] Volkov, R. S., *et al.*, The Influence of Initial Sizes and Velocities of Water Droplets on Transfer Characteristics at High-temperature Gas Flow, *International Journal of Heat and Mass Transfer*, *79* (2014), Dec., pp. 838-845
[7] Volkov, R. S., *et al.*, Experimental Investigation of Mixtures and Foreign Inclusions in Water Droplets Influence on Integral Characteristics of Their Evaporation during Motion Through High-Temperature Gas Area, *International Journal of Thermal Science*, *88* (2015), Feb., pp. 193-200
[8] Gao, Q., *et al.*, Review on Development of Volumetric Particle Image Velocimetry, *Chinese Science Bulletin*, *58* (2013), 36, pp. 4541-4556
[9] Kawaguchi, T., *et al.*, Size Measurements of Droplets and Bubbles by Advanced Interferometric Laser Imaging Technique, *Measurement Science and Technology*, *13* (2002), 3, pp. 308-316
[10] Akhmetbekov, Y. K., *et al.*, Planar Fluorescence for Round Bubble Imaging and its Application for the Study of an Axisymmetric Two-phase Jet, *Experiments in Fluids*, *48* (2010), 4, pp. 615-629
[11] Zhang, X. B., *et al.*, Effects of Surface Tension on Bubble Growth in an Extensive Uniformly Superheated Liquid, *Chinese Science Bulletin*, *56* (2011), 30, pp. 3191-3198
[12] Aoki, J., *et al.*, Mass Transfer from Single Carbon Dioxide Bubbles in Contaminated Water in a Vertical Pipe, *International Journal of Heat and Mass Transfer*, *83* (2015), Apr., pp. 652-658
[13] Santangelo, P. E., Experiments and Modeling of Discharge Characteristics in Water-mist Sprays Generated by Pressure-Swirl Atomizers, *Journal of Thermal Science*, *21* (2012), 6, pp. 539-548
[14] Varaksin, A. Yu., Fluid Dynamics and Thermal Physics of Two Phase Flows: Problems and Achievements, *High Temperature*, *51* (2013), 3, pp. 377-407
[15] Strizhak, P. A., Influence of Droplet Distribution in a "Water Slug" on the Temperature and Concentration of Combustion Products in its Wake, *Journal of Engineering Physics and Thermophysics*, *86* (2013), 4, 895-904

[16] Kuznetsov, G. V., Strizhak, P. A., Numerical Investigation of the Influence of Convection in a Mixture of Combustion Products on the Integral Characteristics of the Evaporation of a Finely Atomized Water Drop, *Journal of Engineering Physics and Thermophysics*, *87* (2014), 1, pp. 103-111
[17] Kuznetsov, G. V., *et al.*, Estimation of the Numerical Values of the Evaporation Constants of the Water Drops Moving in the High Temperature Gas Flow, *High Temperature*, *53* (2015), 2, pp. 254-258
[18] Kuznetsov, G. V., Strizhak, P. A., Analysis of Possible Reasons for Macroscopic Differences in the Characteristics of the Ignition of a Model Liquid Fuel by a Local Heat Source and a Massive Heated Body, *Russian Journal of Physical Chemistry B*, 6 (2012), 4, pp. 498-510
[19] Samarskii, A. A., *The Theory of Difference Schemes*, Marcel Dekker Inc., New York, USA, 2001
[20] Kothandaraman, C., Subramanyan, S., *Heat and Mass Transfer Data Book*, Halsted Press/Wiley, Hoboken, New York, USA, 1975
[21] Wong, H. Y., *Handbook of Essential Formulae and Data on Heat Transfer for Engineers*, Longman Group, London, UK, 1977
[22] Vargaftik, N. B., *et al.*, *Handbook of Thermal Conductivity of Liquids and Gases*, CRC Press, Inc., Boca Raton, Fla., USA, 1994

Paper submitted: April 18, 2015
Paper revised: October 5, 2015
Paper accepted: October 24, 2015